

Coliform removal efficacy of polyurethane foam impregnated with chitosan nanoparticles and silver/silver oxide nanoparticles

Anjali P. Sasidharan^a, Meera V^{a,*} and Vinod P. Raphael^b

^a Department of Civil Engineering, Government Engineering College, Thrissur, APJ Abdul Kalam Technological University, Kerala, India

^b Department of Chemistry, Government Engineering College, Thrissur, APJ Abdul Kalam Technological University, Kerala, India

*Corresponding author. E-mail: vmeera@gectcr.ac.in

ABSTRACT

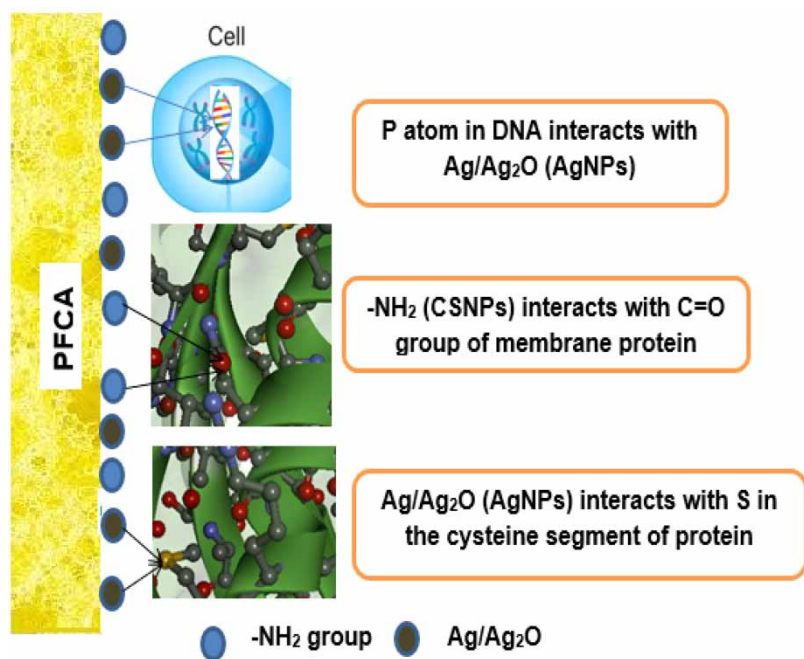
This study was intended to synthesise, characterise and evaluate the antibacterial activity and *Escherichia coli* removal efficacy of a novel polyurethane foam impregnated with nanochitosan and nanosilver/silver oxide (PFCA). The study also exposed the effectiveness of nanochitosan as a disinfectant and as a binder for AgNPs, which has not been explored so far. The *E. coli* removal mechanism and antibacterial activity of PFCA were established by FTIR spectroscopy, XRD pattern and SEM analysis. PFCA achieved complete removal of *E. coli* with sufficient reusing capacities and possessed 100% antibacterial efficiency in a bacterial suspension of 5×10^6 CFU/mL. The study also showed that varying pH from 5 to 9 did not make any significant changes in the removal of *E. coli*. The presence of co-existing ions and organic matter did not reduce the efficiency of PFCA. The elution of silver ions (a very common limitation in treatment processes involving silver ions) was found to be much less, well below the drinking water limit. The study proved excellent potential of PFCA in removing *E. coli*, making it a viable disinfectant for water/wastewater treatment.

Key words: antibacterial activity, *E. coli*, impregnation, nanochitosan, nanosilver/silver oxide, polyurethane foam

HIGHLIGHTS

- Developed a novel and reliable sorbent cum disinfectant, PFCA by loading nanochitosan and nanosilver/silver oxide on PUF.
- PFCA achieved complete removal of coliforms with sufficient reusing capacities.
- The elution of silver ions was found to be much less, well below the drinking water limit.
- Performance was unaffected in the presence of co-existing anions and organic matter.
- No pH adjustment is required.

GRAPHICAL ABSTRACT



INTRODUCTION

Water is a valuable resource that has been egregiously mistreated as a result of the rapid growth in population associated with industrialisation and changes in land use. This leads to water pollution and water scarcity. The ejection of contaminated water to surface water sources results in bacterial pollution. The major sources of microbial pollution include improperly treated sewage, and industrial sources like slaughterhouses and runoff from animal wastes. The microbiological risks depend on the bacterial concentration in water and on the water usage such as drinking, recreational activities, irrigation, and aquaculture purposes (Pachepsky *et al.* 2018). The contamination of water can be monitored by microbial indicators. Coliform bacteria are often considered as the microbial indicators of pathogenic pollution. The coliform bacteria are rod-shaped Gram-negative, non-spore-forming microbes. They are found in the intestine of warm-blooded animals and in soil.

Nowadays the most common procedure adopted for water disinfection is chlorination. Chlorination is effective against waterborne pathogens and can prevent future contamination due to residual effects. However, the compounds of chlorine will result in the production of dangerous disinfection by-products that are carcinogenic (Mazhar *et al.* 2020). The other advanced methods include ozonation and ultraviolet (UV) radiation. For UV light exposure, water must be free from turbidity, colour and odour because they make penetration of radiation difficult and the microorganisms get protection from radiation. Even though UV light is effective in removing microorganisms, it is very costly and requires electricity to work. In the process of ozonation, ozone gas is used. The instability and high reactive chemical properties of ozone gas transform ozone back to oxygen, thus making it less effective (Stanfield *et al.* 2003). This results in an urgent need for the development of new promising materials.

Nanotechnology offers many possibilities for improving the efficiency of water disinfection. Creation, refining and application of materials at a nanoscale furnished effective removal of pathogens due to the higher surface area and reactivity of nanomaterials (Asadi & Moeinpour 2019). From the diverse range of nanomaterials, metal/metal oxides and chitosan offer various advantages for removing bacterial contamination from water/wastewater. Better stability, simple preparation method, low toxicity along with reactive amino and hydroxy groups make chitosan nanoparticles distinct. The effective synthetic methodology for preparing stable metal/metal oxide nanoparticles with high sorption potential holds a central position for their potential use in the treatment of water and wastewater.

Chitosan/chitosan-based nanomaterials have chelating activities, versatility, and stability, increasing their application in various scientific and engineering applications. The chelating ability of nanochitosan with metal ions results in the

establishment of strong complexes with metals (Abd-Elhakeem *et al.* 2016). The metal holding capability of nanochitosan increases its suitability in the field of water/wastewater treatment. They have proved their potential in water/wastewater treatment and were effectively used as an antibacterial agent (Huang *et al.* 2009; Yanat & Schroën 2021). The antibacterial action of metal/metal oxide nanoparticles (silver/silver oxide, copper/copper oxide, titanium/titanium oxide, zinc/zinc oxide) has long been known. Among these metal/metal oxide nanoparticles, silver/silver oxide nanoparticles showed excellence and wide application in the removal of pathogens from water/wastewater (Pathak & Gopal 2012; Bahri *et al.* 2020).

The practical use of the nanoparticles in the treatment of water/wastewater can be enhanced by a suitable support medium. Due to high surface area, open porous structure and capacity to bind nanoparticles, polyurethane foams have been recently used as efficient support media. The immobilisation of nanoparticles on polyurethane foam provides good mechanical stability and easy phase separation (Centenaro *et al.* 2017; Khan *et al.* 2019).

Thus, the combination of nanochitosan and nanosilver/silver oxide impregnated on polyurethane foam will result in the formation of a stable, favourable and efficient disinfectant. Also, the reactive amino group of nanochitosan can act as a binder for silver/silver oxide nanoparticles. This avoids the need of additional binder, making the process more economical.

The main objective of the present work was to investigate the potency of nanochitosan and nanosilver/silver oxide impregnated polyurethane foam (PFCA) in the removal of *Escherichia coli* from the aqueous solution. The sorbent characterisation was done using field emission scanning electron microscopy (FESEM), point of zero charge, Fourier transform infrared (FTIR) spectroscopy, Brunauer–Emmett–Teller (BET) studies, X-ray diffraction (XRD) studies, and inductively coupled plasma optical emission spectroscopy (ICP-OES). The influence of contact time, dosage of sorbent, pH, initial concentration, co-existing anions and organic matter, and reuse capacity of sorbents in removing *E. coli* from aqueous solutions was investigated. The antibacterial activity of PFCA was also assessed.

MATERIALS AND METHODS

Materials

The study was carried out using chemicals of analytical quality. The reagents potassium dihydrogen phosphate (KH_2PO_4), nitric acid (HNO_3), sodium hydroxide (NaOH), silver nitrate, hydrochloric acid (HCl), sodium bicarbonate (NaHCO_3), sodium tripolyphosphate ($\text{Na}_2\text{P}_3\text{O}_{10}$), sodium sulphate (Na_2SO_4), sodium chloride (NaCl), sodium nitrate (NaNO_3), humic acid, glucose, nutrient broth, plate count agar and M-Endo medium were provided by Merck Millipore. The *Escherichia coli* culture was obtained from the College of Veterinary and Animal Sciences, Mannuthy, Kerala, India. Chitosan (extra pure, medium MW) was procured from Sisco Research Laboratories Pvt. Ltd

Methodology

The schematic representation of the methodology adopted in the study is shown in Figure 1.

Synthesis of nanoparticles and fabrication of sorbent

Nanochitosan (CSNPs) was prepared by crosslinking chitosan (CS) with sodium tripolyphosphate (TPP) as per the methods suggested by many researchers (Agarwal *et al.* 2018; Anand *et al.* 2018). The stable silver/silver oxide nanoparticles (AgNPs) was prepared by treating silver nitrate with chitosan as mentioned by several investigators (Venkatesham *et al.* 2014; Kalai-vani *et al.* 2018).

The wet impregnation method was used for preparing the sorbent (Centenaro *et al.* 2017; Khan *et al.* 2019). The washed and dried polyurethane foam (PUF of size $50 \times 50 \times 6$ mm) was immersed in CSNPs solution for 24 h. Then PUFs coated with CSNPs were soaked in AgNPs solution for 24 h and allowed for solvent evaporation. The obtained PFCA was washed, dried and stored for future use.

Characterisation techniques

The advent of nanoparticles was ensured by studying the UV-Vis spectrum in the range of 200–600 nm using spectrophotometer (Systronics 2202). The size and shape of nanoparticles were verified by the FESEM (field emission scanning electron microscope) images acquired from HITACHI SU 6600. The characteristic functional groups on PFCA (before and after treatment) were detected using the FTIR (Fourier transform infrared) spectrum in the range of $500\text{--}4000\text{ cm}^{-1}$ taken by the spectrometer, Thermo Nicolet Avtar 370. The crystalline and non-crystalline nature of nanoparticles and PFCA was assessed using XRD (X-ray diffraction) patterns in the range of $10\text{--}80^\circ$, recorded by Rigaku Ultima IV

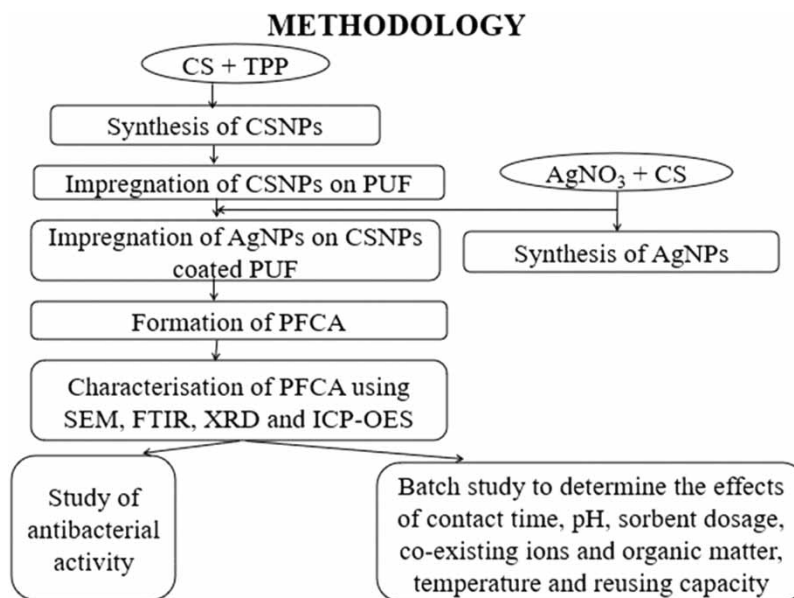


Figure 1 | Flowchart of methodology.

diffractometer (Cu $K\alpha$ radiation, $\lambda = 1.54060\text{\AA}$ at $25\text{ }^\circ\text{C}$). The BET (Brunauer–Emmett–Teller) analysis using Belsorp Max, Microtrac Belcorp, Japan, determined the surface area and pore volume of PFCA. The surface charge of PFCA was assessed by measuring the point of zero charge (Ahmad & Kumar 2010). ICP-OES (inductively coupled plasma optical emission spectroscopy) using ICAP 7000 Series evaluated the amount of silver ions coated on PUF and in the effluent after treatment with PFCA.

Preparation and analysis of synthetic *E. coli* suspension

For avoiding any contamination, all apparatus and glasswares were sterilized by autoclaving at $121\text{ }^\circ\text{C}$ for 15 minutes before use. The nutrient broth solution for culturing *E. coli* was prepared by suspending 13 g of nutrient broth in 1000 mL of distilled water. It was then heated until the media was dissolved completely. The media was sterilized by autoclaving at 6.8 kg ($121\text{ }^\circ\text{C}$) for 15 minutes. One mL of the *E. coli* culture was transferred to 50 mL of nutrient broth solution and incubated at $37\text{ }^\circ\text{C}$ for 24 h. The excess nutrient broth was removed by centrifugation and the *E. coli* culture was stored in the cold. The bacterial count was determined using the membrane filter technique using M-Endo medium and agar (APHA 2017). The synthetic wastewater was prepared by adding *E. coli* bacterial culture to the sterile distilled water and diluted to obtain the desired concentrations of 10^3 , 10^4 , 10^5 and 10^6 CFU/mL.

Study of antibacterial activity

The antibacterial activity of the sorbents was assessed by measuring the optical density of broth solutions (inoculated with bacterial feed) containing sorbents in the UV-Vis spectrophotometer at 600 nm (Waheed *et al.* 2014). The wavelength of light for determining optical density is 600 nm because it is much less phototoxic and also organic materials readily absorb this light. The nutrient broth was prepared and 40 mL of nutrient broth was added in four conical flasks of 250 mL capacity. All flasks were autoclaved at $121\text{ }^\circ\text{C}$ for 15 min before use. One flask with nutrient broth alone without bacterial feed was used as blank. The other three flasks were inoculated with 1 mL of prepared bacterial suspension (5×10^6 CFU/mL). The sorbents PUF, and PFCA (0.6 g) were introduced in each flask and one flask was kept without sorbents. All flasks were incubated at $35 \pm 0.5\text{ }^\circ\text{C}$ in an incubator for 18 h. After incubation, optical densities (OD) of suspensions were taken using the spectrophotometer at 600 nm.

Batch study for the evaluation of *E. coli* removal efficacy of the sorbents

The effect of various factors like contact time, adsorbent dosage, pH of the medium, and influent concentration on the removal of *E. coli* were studied at room temperature ($27\text{ }^\circ\text{C}$). The *E. coli* removal efficacy by varying the temperature was

also investigated. All experiments were done in triplicate with synthetic solutions of volume 200 mL. The reuse capacity of the sorbents was examined. Removal efficiency of *E. coli* (%) is given by:

$$E = \frac{(C_0 - C_t)}{C_0} \times 100 \quad (1)$$

where C_0 and C_t are the bacterial concentration at initial and at any time t in CFU/mL respectively.

Effect of contact time and pH

The impact of contact time on removing *E. coli* was examined for 0.5–3 h (0.5 h interval) and 24 h by keeping the sorbent dosage at 3 g/L, influent concentration of 38×10^5 CFU/mL (concentration in low strength greywater – Al-Gheethi *et al.* 2016) and pH 6 as constant. The impact of pH on removing *E. coli* was estimated by tuning the pH of the solution from 5 to 9 using 1N HCl and 1N NaOH for different contact times (0.5–3 h).

Effect of sorbent dosage and initial *E. coli* concentration

The effects of initial *E. coli* concentration on removing *E. coli* were studied by varying concentrations from 10^5 to 10^6 CFU/mL (range of concentration present in greywater) and dosage of PFCA for each concentration from 1 to 7 g/L at optimised pH and equilibrium time.

Effect of co-existing ions and organic matter

The impact of co-existing ions like HCO_3^- , Cl^- , NO_3^- , PO_4^{3-} and SO_4^{2-} on removing *E. coli* were observed by mixing the synthetic bacterial suspension with the solutions of known concentration (100, 150, 200 and 250 mg/L – concentration representing greywater) of these ions one at a time. The effects of co-existing organic matter on removing *E. coli* were studied by using glucose and humic acid. The humic acid/glucose was mixed in synthetic *E. coli* solution to obtain total organic carbon (TOC) concentration of 50, 100, 500 and 1000 mg C/L (concentration representing greywater – Satyanarayana *et al.* 2015). The efficacy of the sorbent in removing *E. coli* in the presence of co-existing ions and organic matter was conducted at optimised values of adsorbent dosage, pH, and contact time for an influent *E. coli* concentration of 5×10^6 CFU/mL.

Effect of temperature

The impact of temperature was investigated by varying temperature from 20 to 40 °C (at an interval of 10 °C) for an influent *E. coli* concentration of 5×10^6 CFU/mL at optimised values of pH, adsorbent dosage, and contact time.

Reusing capacity of sorbents

The reusing capability of sorbent was investigated as a batch process. For this, the adsorbent was removed from the medium and reintroduced into a new solution (5×10^6 CFU/mL) without cleaning and the *E. coli* removal efficiency was found at optimised values of pH, contact time and adsorbent dosage. The reusing capacity of the sorbent after treating with 0.5 M NaOH for 24 h was also evaluated.

RESULTS AND DISCUSSION

Sorbent characterisation

The UV-Vis spectrum of CSNPs and AgNPs provided the highest absorbance peak at 280 and 433 nm respectively. The FESEM images conveyed the size of CSNPs in the range of 56–112 nm and AgNPs in the range of 44–75 nm. The FESEM images of CSNPs, AgNPs, PUF, and PFCA are shown in Figure S1A, B, C, and D respectively in the supplementary information. The nanoparticles were spherical in shape and proved their agglomeration in the FESEM images (S1A and B). The impregnation of CSNPs and AgNPs on PUF increased their stability by preventing agglomeration (S1D). The interplay of characteristic functional groups for the emergence of CSNPs, AgNPs, and PFCA was exposed by IR spectroscopic examinations. The IR spectra of CS, CSNPs, AgNPs, and PUF are displayed in Figure S2A, B, C, and D in the supplementary information. The IR spectroscopic examinations demonstrated the holding of CSNPs by the N-H group of PUF, followed by the binding of AgNPs by amino group of CSNPs and carbamate group of PUF to form PFCA (Figure 6(a)). The non-

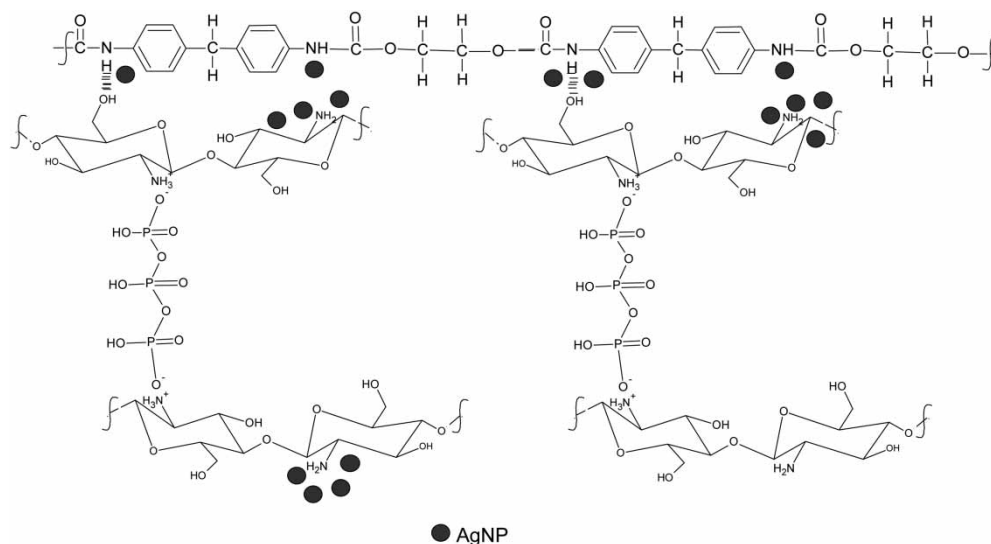


Figure 2 | Structure of PFCA.

crystalline nature of CSNPs and crystalline nature of AgNPs was indicated by the XRD pattern of PFCA (Figure 6(b)). The XRD patterns of CSNPs (Figure S3A), AgNPs (Figure S3B), and PUF (Figure S3C) are included in the supplementary section.

The BET studies presented the surface area of PUF as 1.36 m²/g and an increased value of 2.17 m²/g upon impregnation with nanoparticles. The point of zero charge measurement exhibited the positive surface charge of PFCA below pH 7.7. The plots of BET analysis (Figure S4) and point of zero charge (Figure S5) are included in the supplementary information. The amount of silver ions coated on PFCA was found to be 5.69 g/kg in the ICP-OES analysis. The microscopic and spectroscopic analysis, XRD studies and BET analysis of PFCA were conveyed in the former study (Sasidharan *et al.* 2021). The structure of PFCA is shown in Figure 2.

Antibacterial activity of PUF and PFCA

In the antibacterial assay test it was observed that the sample containing PUF was turbid and that of PFCA was clear. The turbidity is proportional to the number of *bacteria* (Farrell *et al.* 2018) and the optical density (OD) values can be used to quantify the results. The absorbance of light will be higher in the samples with greater bacterial concentrations (Waheed *et al.* 2014). The OD values at 600 nm were 1.455 for the inoculated bacterial suspension, 1.390 for the inoculated bacterial suspension with PUF, and 0.000 for the inoculated bacterial suspension with PFCA. The results showed 100% antibacterial activity for PFCA and the inactivation of bacterial growth by PUF was only 2.41%. The excellent antibacterial property of PFCA is due to the presence of CSNPs and AgNPs.

Studies on the removal of *E.coli* under batch mode

Effect of contact time

The performance of PFCA was assessed at room temperature (27 °C) with pH 6, influent *E. coli* concentration of 38 × 10³ CFU/mL, and adsorbent dosage 3 g/L. The *E. coli* removal efficacy of PFCA increased with time and reached equilibrium at 1.5 h (Figure 3(a)). This was because effective reaction time is needed for the bacterial cell membranes to interact with the nanoparticles on the sorbent surface. No substantial changes were observed beyond 1.5 h. Within 1.5 h, PFCA achieved complete removal of *E. coli*. Table S1 in the supplementary information provides the impact of contact time on removing *E. coli* by PFCA.

Effect of pH

The *E. coli* removal efficacy of PFCA was monitored at 27 °C (room temperature) by varying the pH of the solution from 5 to 9 for different contact times (0.5–3 h). The quantity of PFCA (3 g/L) and *E. coli* concentration (38 × 10³ CFU/mL) were retained

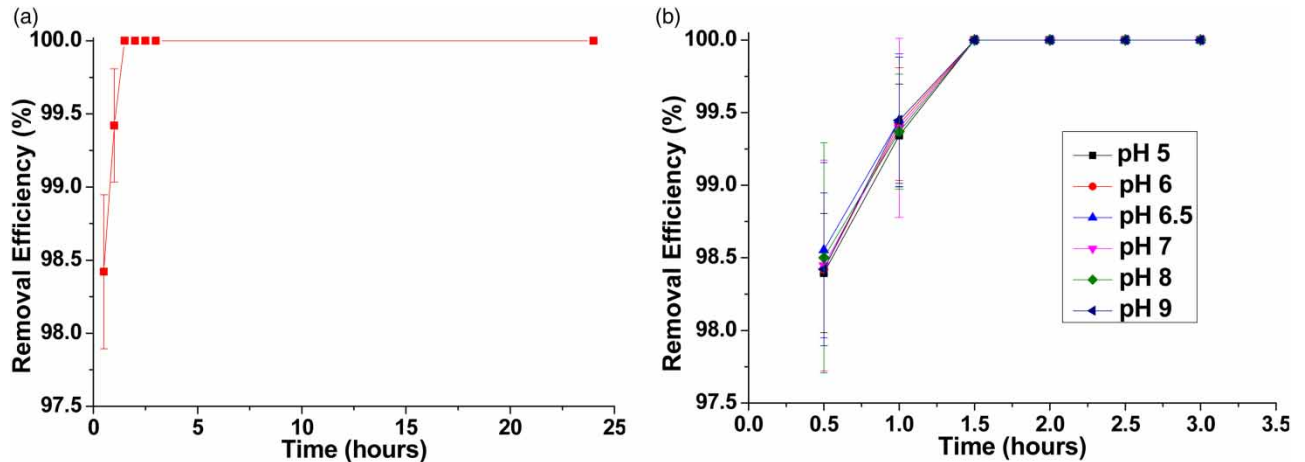


Figure 3 | Effect of (a) contact time (pH 6, influent *E. coli* concentration of 38×10^3 CFU/mL, and adsorbent dosage 3 g/L) and (b) pH (influent *E. coli* removal concentration of 38×10^3 CFU/mL, and adsorbent dosage 3 g/L) on *E. coli* removal by PFCA.

for all these runs. The influence of pH on the removal of *E. coli* by PFCA is depicted in Figure 3(b) and the values of residual *E. coli* concentration along with removal efficiency are shown in Table S2 in the supplementary information.

The results show that varying pH from 5 to 9 did not make any significant changes in the *E. coli* removal efficacy. Similar observation was reported in removing *E. coli* using silver-coated $\text{Ni}_{0.5}\text{Zn}_{0.5}\text{Fe}_2\text{O}_4$ and this study conveyed that the intestinal bacteria were not amenable to pH changes from 5 to 9 (Asadi & Moeinpour 2019). At all pH, the bacterial count in the effluent after treatment with PFCA was nil (bacteria undetected) within 1.5 h. This adds to the advantage of application of PFCA in water/wastewater treatment.

Effect of adsorbent dosage and influent *E. coli* concentration

The impact of influent *E. coli* concentration was examined by changing the concentration from 10^3 to 10^6 CFU/mL and dosage of PFCA for each *E. coli* concentration from 1 to 7 g/L at contact time 1.5 h and pH 6.5. The *E. coli* removal efficacy increased with the increase in sorbent dosage. This was due to the availability of more nanoparticles to contact with bacteria resulting in more antibacterial activity and thus intensifying the removal of *E. coli*. But However, increasing the amount of PFCA beyond optimum dosage for a particular concentration did not result in a substantial increase in the removal of *E. coli*. The bacterial count after treatment with PFCA remained nil for each *E. coli* concentration at optimum dosage (3 g/L for 10^3 CFU/mL, 4 g/L for 10^4 CFU/mL, 4 g/L for 10^5 CFU/mL, and 5 g/L for 10^6 CFU/mL). The results are depicted in Figure 4 and Table S3 in the supplementary information.

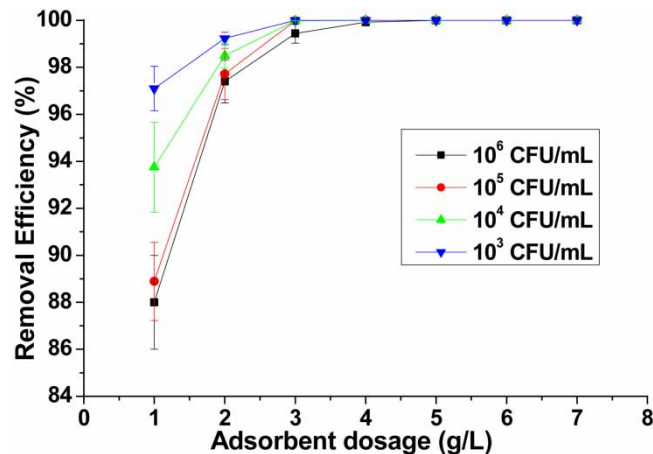


Figure 4 | Effect of influent *E. coli* concentration and adsorbent dosage on *E. coli* removal by PFCA (contact time 1.5 h and pH 6.5).

Impact of co-existing ions and organic matter on the removal of *E. coli* by PFCA

The effects of co-existing anions (Cl^- , HCO_3^- , NO_3^- , PO_4^{3-} and SO_4^{2-}) with concentrations from 100 to 250 mg/L, and organic matter (humic acid and glucose) with concentrations from 50 to 1000 mg C/L on *E. coli* removal by PFCA were examined for an influent *E. coli* concentration of 5×10^6 CFU/mL. The operating parameters were contact time 1.5 h, pH 6.5 and adsorbent dosage 5 g/L. The results show that the presence of higher or lower concentrations of co-existing ions and organic matter did not influence the removal of *E. coli* by PFCA and bacteria were undetected in all cases, making it suitable for removing *E. coli* from wastewater.

Effect of temperature on the *E. coli* removal efficacy of PFCA

The study was conducted at different temperatures (20, 30 and 40 °C) with pH 6.5, influent concentration 5×10^6 CFU/mL, contact time 1.5 h, and sorbent dosage 5 g/L (Table 1). The results showed that the bactericidal activity of PFCA was reduced below room temperature (RT) of 27 °C. The effectiveness in killing microorganisms by chemical disinfectants like silver will decrease at low temperatures (Pathak & Gopal 2012).

Reusing capacity of PFCA

PFCA was reused without any pre-treatment before the new run. The reusing capability of sorbents was evaluated by keeping operational parameters as contact time 1.5 h, pH 6.5, influent *E. coli* concentration 5×10^6 CFU/mL and adsorbent dosage 5 g/L. *E. coli* were undetected in the aqueous solution up to three reuse cycles. Thereafter, a decrease in the removal of *E. coli* was observed and 94% removal efficiency was obtained in the seventh reuse cycle. This ability increases the suitability of PFCA as an effective adsorbent to remove *E. coli*. The reuse capability of PFCA is shown in Figure 5 and Table S4 in the supplementary information.

PFCA showed reduced efficacy in removing *E. coli* after the third reuse cycle. Hence to verify any enhancement in the performance of PFCA in removing *E. coli* after the third reuse cycle, PFCA was treated with 0.5 M NaOH solution for 24 h to

Table 1 | Effect of temperature on *E. coli* removal by PFCA

Temperature (°C)	Residual concentration (CFU/mL)	Removal efficiency (%)
20	300	99.99
30	Below detectable level	~ 100
40	Below detectable level	~ 100

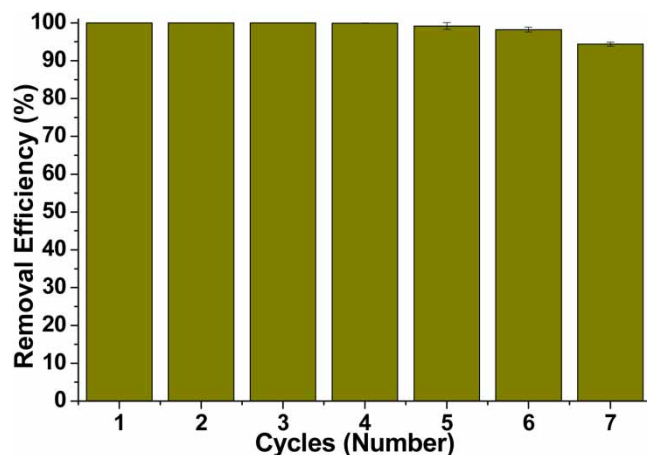


Figure 5 | *E. coli* removal efficiency of PFCA with reuse cycles (contact time 1.5 h, pH 6.5, influent concentration 5×10^6 CFU/mL and adsorbent dosage 5 g/L).

denature the bacterial DNA and remove any dead cells from the sorbent surface. The NaOH can break the hydrogen bonds between DNA molecules and denature it (Wang *et al.* 2014). However, no change in percentage efficiency in removing *E. coli* was observed.

The usage of amino groups and silver ions for disinfecting bacteria in each cycle of treatment reduces the efficacy of PFCA in removing *E. coli*. The interactive effects of nanoparticles with microorganisms reduces the antibacterial activity with time (Chen *et al.* 2016).

Silver in treated water

The ICP-OES analysis reported very less leaching of silver ions from PFCA. After the first cycle of treatment and seventh cycle of treatment using PFCA, the effluent silver ion concentrations were 0.08 and 0.009 mg/L respectively. The silver ions concentration in the effluent (<0.10 mg/L) met the WHO standards.

Mechanism of *E. coli* removal by PFCA

The electrostatic sorption of bacterial cell membrane proteins/DNA by the amino group of nanochitosan and silver ions of AgNPs has led to the removal of *E. coli* and antibacterial activity of PFCA, and was established by FTIR spectroscopy, XRD pattern and SEM analysis. The amino groups of CSNPs interact with the carbonyl group (C = O) of cell membrane proteins and disrupt the cell membrane resulting in increased cell membrane permeability and the death of bacteria (Chandrasekaran *et al.* 2020; Yanat & Schroën 2021). The FTIR spectrum of PFCA after *E. coli* removal (Figure 6(a)) showing the vanishing of band at 3279.25 cm^{-1} and the emergence of a new broad band at 3315.41 cm^{-1} , is pinned to the interaction between amino group and the bacterial cell membrane.

The silver ions of AgNPs interact with the phosphorus of DNA and inhibit DNA replication. This inhibition leads to the death of bacteria (Tao *et al.* 2021). The role of silver ions bound to the amino group of CSNPs (Ag-NH) on the surface of PFCA in removing *E. coli* is verified by the vanishing N-H bending vibration denoted by the peak at 808.20 cm^{-1} in the FTIR spectrum of PFCA after treatment. The silver ions of AgNPs also interact with the thiol groups in bacteria proteins to form silver-thiol complex (Ag-S) leading to the elimination of thiol group (Li *et al.* 2016). The new strong band that appears at 505.51 cm^{-1} in the FTIR spectrum of PFCA after *E. coli* removal represents the formation of Ag-S bond. The thiol group (in the cysteine segment) in *E. coli* can be identified by the peak representing S-H stretching vibration at 2550 cm^{-1} in the FTIR spectrum (Li *et al.* 2016). However, the FTIR spectrum taken after *E. coli* removal has no peak representing the thiol group. This again confirms the formation of Ag-S bond. The thiol groups are responsible for the disulphide bond formation in the bacterial cell, which are needed for the proper functioning of proteins. Ag-S formation

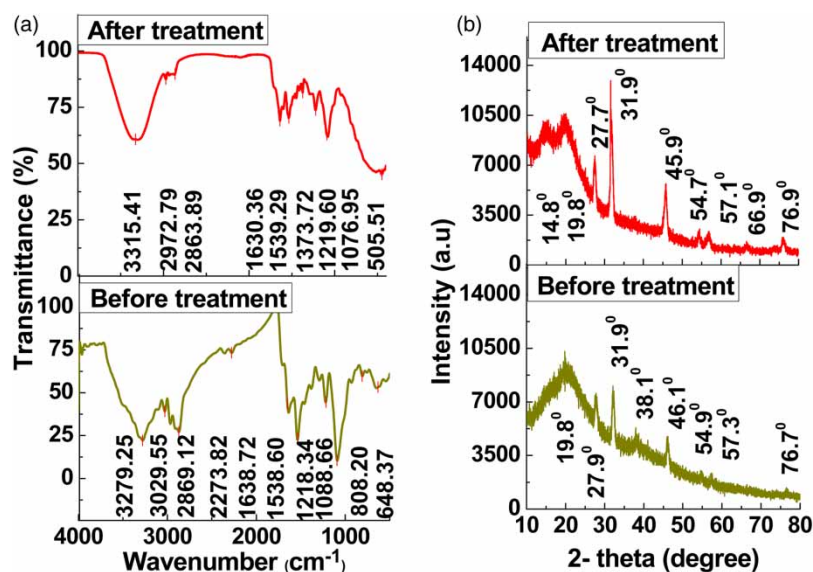


Figure 6 | (a) FTIR spectra and (b) XRD patterns of PFCA before and after treatment.

thus resulted in the interruption of disulphide bond formation and the inactivation of proteins finally leading to the death of *E. coli*.

The XRD result after the removal of *E. coli* by PFCA is depicted in Figure 6(b). The XRD pattern of PFCA after the removal of *E. coli* showed reduction in the peak width represented by the full width at half maximum (FWHM). This established the interaction of silver in eliminating *E. coli*. The changes in the values of FWHM before and after the removal of *E. coli* are given in Table 2.

The surface morphology of PUF and PFCA after treatment (Figure 7(a) and 7(b)) were obtained from SEM images. The regular rod-shaped structure seen on the surface of PUF indicates the presence of live cells of *E. coli*. However, on the surface of PFCA, live or dead cells could not be observed. This indicates the excellent antibacterial activity of PFCA and the sloughing of the dead cells of *E. coli*.

CONCLUSIONS

The present study aimed to develop a simple, compact, reliable and efficient treatment method for removing *E. coli* from aqueous solutions by impregnating chitosan nanoparticles and silver/silver oxide nanoparticles on polyurethane foam (PFCA). The sorbent characterisation by FESEM image and XRD pattern verified the existence of crystalline AgNPs and non-crystalline CSNPs. The FTIR spectroscopic analysis proved that the *E. coli* removal efficacy by PFCA was due to the interaction of amino groups and silver ions on the negatively charged bacterial cell surface. The SEM images supported the bactericidal property of PFCA. The results from the study demonstrated excellent antibacterial activity and *E. coli* removal efficacy of

Table 2 | FWHM values of AgNPs in the XRD peaks of PFCA before and after the removal of *E. coli*

Peak (degrees)	FWHM (degrees)	
	Before treatment	After treatment
27.9	0.423	0.259
31.9	0.475	0.33
46.1	0.78	0.57

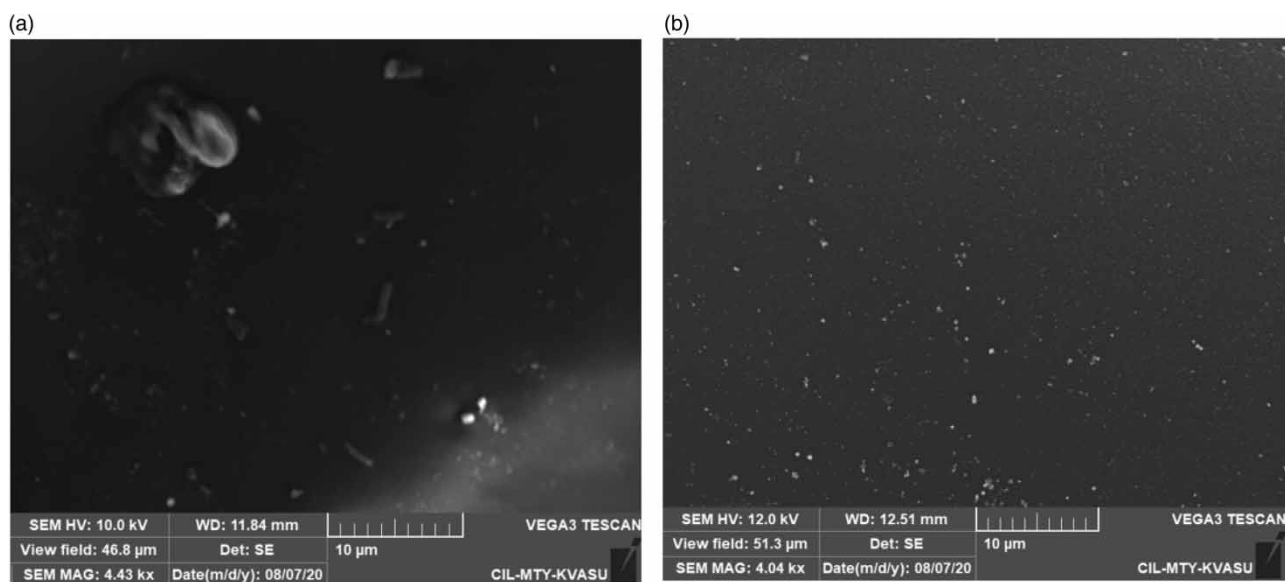


Figure 7 | SEM images after treatment (a) PUF and (b) PFCA.

PFCA. *E. coli* were undetected after treatment by PFCA at all initial concentrations (10^3 – 10^6 CFU/mL). The interactive effects of nanoparticles with microorganisms decrease with each cycle of reuse. This resulted in reduced removal efficacy after the third reuse cycle. Analysis of effluent after treatment with PFCA by ICP-OES technique indicated extremely low presence of silver ions, less than the permissible limit in drinking water. This indicated the effective bonding of AgNPs on PUF in the presence of CSNPs, which was due to the presence of reactive amino groups of CSNPs. The amino group of CSNPs can form a stable complex with silver ions and thereby act as a feasible eco-friendly binder for AgNPs on PUF. The bacterial removal efficiency by PFCA remained unchanged in the presence of co-existing anions and organic matter. Influent pH did not affect the *E. coli* removal in the pH range studied (pH 5–9). These abilities of PFCA increase its suitability in water/wastewater treatment. The effluent from PFCA can be used for potable purpose in terms of *E. coli*. The cost of silver nanoparticles is one of the restraints of the study. This can be overlooked by its unaffected and excellent *E. coli* removal efficiency in the presence of competing ions and reusing capability.

ACKNOWLEDGEMENTS

The authors would like to thank the laboratory staff and co-researcher at Government Engineering College, Thrissur, Kerala for their help and support. The facilities arranged by the C-MET, Thrissur and STIC, Cochin as part of characterization studies are strongly appreciated.

ETHICS APPROVAL

Not applicable

CONSENT TO PARTICIPATE

Not applicable

CONSENT FOR PUBLICATION

Not applicable

AVAILABILITY OF DATA AND MATERIAL

This research article and supplementary information file contain all the data generated or analysed during this study.

CONFLICTS OF INTEREST/COMPETING INTERESTS

The authors declare that they have no potential competing interests.

FUNDING

The authors did not receive any financial support for the submitted work.

AUTHORS CONTRIBUTIONS

Conceptualization, Methodology, Formal analysis and investigation, Writing – Original Draft were performed by Anjali P. Sasidharan. Writing – Review & Editing, Supervision was performed by Meera V and Vinod P. Raphael. The manuscript was read and approved by all authors.

DATA AVAILABILITY STATEMENT

All relevant data are included in the paper or its Supplementary Information.

REFERENCES

Abd-Elhakeem, M. A., Ramadan, M. M. & Basaad, F. S. 2016 *Removing of heavy metals from water by chitosan nanoparticles. Journal of Advances in Chemistry* **11** (7), 3765–3771. <https://doi.org/10.24297/jac.v11i7.2200>.

- Agarwal, M., Agarwal, M. K., Shrivastav, N., Pandey, S., Das, R. & Gaur, P. 2018 Preparation of chitosan nanoparticles and their in-vitro characterization. *International Journal of Life-Sciences Scientific Research* **4** (2), 1713–1720. <https://doi.org/10.21276/ijlssr.2018.4.2.17>.
- Ahmad, R. & Kumar, R. 2010 Adsorption studies of hazardous malachite green onto treated ginger waste. *Journal of Environmental Management* **91** (4), 1032–1038. <http://dx.doi.org/10.1016/j.jenvman.2009.12.016>.
- Al-Gheethi, A. A., Mohamed, R. M. S. R., Bala, J. D., Efaq, A. N. & Hazim, M. K. A. 2016 Reduction of microbial risk associated with greywater by disinfection processes for irrigation. *Journal of Water and Health* **14** (3), 379–398. <https://doi.org/10.2166/wh.2015.220>.
- Anand, M., Sathyapriya, P., Maruthupandy, M. & Hameedha Beevi, A. 2018 Synthesis of chitosan nanoparticles by TPP and their potential mosquito larvicidal application. *Frontiers in Laboratory Medicine* **2** (2), 72–78. <https://doi.org/10.1016/j.flm.2018.07.003>.
- APHA, A.W 2017 *Standard Methods for the Examination of Water and Wastewater*, 23rd edn. Am. Public Heal. Assoc. (APHA), Am. Water Work. Assoc. (AWWA), Water Environ. Fed. (WEF), Washingt, DC, USA.
- Asadi, S. & Moeinpour, F. 2019 Inactivation of *Escherichia coli* in water by silver-coated Ni_{0.5}Zn_{0.5}Fe₂O₄ magnetic nanocomposite: a Box–Behnken design optimization. *Applied Water Science* **9** (1), 1–9. <https://doi.org/10.1007/s13201-019-0901-4>.
- Bahri, M., Hamidian, A. H., Zhang, Y. & Yang, M. 2020 Removal of coliform bacteria from dairy wastewater using graphene-silver nanocomposite. *International Journal of Aquatic Biology* **8**, 447–454. <https://doi.org/10.22034/ijab.v8i6.1025>.
- Centenaro, G. S. N. M., Facin, B. R., Valério, A., de Souza, A. A. U., da Silva, A., de Oliveira, J. V. & de Oliveira, D. 2017 Application of polyurethane foam chitosan-coated as a low-cost adsorbent in the effluent treatment. *Journal of Water Process Engineering* **20**, 201–206. <http://dx.doi.org/10.1016/j.jwpe.2017.11.008>.
- Chandrasekaran, M., Kim, K. D. & Chun, S. C. 2020 Antibacterial activity of chitosan nanoparticles: a review. *Processes* **8**, 1–21. <http://dx.doi.org/10.3390/pr8091173>.
- Chen, J., Li, S., Luo, J., Wang, R. & Ding, W. 2016 Enhancement of the antibacterial activity of silver nanoparticles against phytopathogenic bacterium *Ralstonia solanacearum* by stabilization. *Journal of Nanomaterials* **2016**, 1–15. <http://dx.doi.org/10.1155/2016/7135852>.
- Farrell, C., Hassard, F., Jefferson, B., Leziart, T., Nocker, A. & Jarvis, P. 2018 Turbidity composition and the relationship with microbial attachment and UV inactivation efficacy. *Science of the Total Environment* **624**, 638–647. <https://doi.org/10.1016/j.scitotenv.2017.12.173>.
- Huang, L., Cheng, X., Liu, C., Xing, K., Zhang, J., Sun, G., Li, X. & Chen, X. 2009 Preparation, characterization, and antibacterial activity of oleic acid-grafted chitosan oligosaccharide nanoparticles. *Frontiers in Biology* **4**, 321–327. <https://doi.org/10.1007/s11515-009-0027-4>.
- Kalaivani, R., Maruthupandy, M., Muneeswaran, T., Beevi, A. H., Anand, M., Ramakritinan, C. M. & Kumaraguru, A. K. 2018 Synthesis of chitosan mediated silver nanoparticles (AgNPs) for potential antimicrobial applications. *Frontiers in Laboratory Medicine* **2** (1), 30–35. <https://doi.org/10.1016/j.flm.2018.04.002>.
- Khan, M. S. J., Kamal, T., Ali, F., Asiri, A. M. & Khan, S. B. 2019 Chitosan-coated polyurethane sponge supported metal nanoparticles for catalytic reduction of organic pollutants. *International Journal of Biological Macromolecules* **132**, 772–783. <https://doi.org/10.1016/j.ijbiomac.2019.03.205>.
- Li, H., Gao, Y., Li, C., Ma, G., Shang, Y. & Sun, Y. 2016 A comparative study of the antibacterial mechanisms of silver ion and silver nanoparticles by Fourier transform infrared spectroscopy. *Vibrational Spectroscopy* **85**, 112–121. <http://dx.doi.org/10.1016/j.vibspec.2016.04.007>.
- Mazhar, M. A., Khan, N. A., Ahmed, S., Khan, A. H., Hussain, A., Rahisuddin Changani, F., Yousefi, M., Ahmadi, S. & Vambol, V. 2020 Chlorination disinfection by-products in municipal drinking water – a review. *Journal of Cleaner Production* **273**, 1–13. <https://doi.org/10.1016/j.jclepro.2020.123159>.
- Pachepsky, Y. A., Allende, A., Boithias, L., Cho, K., Jamieson, R., Hofstra, N. & Molina, M. 2018 Microbial water quality: monitoring and modeling. *Journal of Environmental Quality* **47**, 931–938. <https://doi.org/10.2134/jeq2018.07.0277>.
- Pathak, S. P. & Gopal, K. 2012 Evaluation of bactericidal efficacy of silver ions on *Escherichia coli* for drinking water disinfection. *Environmental Science and Pollution Research* **19** (6), 2285–2290. <https://doi.org/10.1007/s11356-011-0735-6>.
- Sasidharan, A. P., Meera, V. & Raphael, V. P. 2021 Investigations on characteristics of polyurethane foam impregnated with nanochitosan and nanosilver/silver oxide and its effectiveness in phosphate removal. *Environmental Science and Pollution Research* **28** (10), 12980–12992. <https://doi.org/10.1007/s11356-020-11257-2>.
- Satyanarayana, S. V., Varghese, M., Feroz, S. & Rao, L. N. 2015 Total organic carbon and its variation in grey water samples. *International Journal of Applied Research*. 7-573-575. <https://doi.org/10.13140/RG.2.1.2558.0647>
- Stanfield, G., Lechevallier, M. & Snozzi, M. 2003 Treatment efficiency in assessing microbial safety of drinking water. *Improving Approaches and Methods*, 159–178. <https://doi.org/10.1787/9789264099470-en>.
- Tao, Y., Aparicio, T., Li, M., Leong, K. W., Zha, S. & Gautier, J. 2021 Inhibition of DNA replication initiation by silver nanoclusters. *Nucleic Acids Research* **49** (9), 5074–5083. <https://doi.org/10.1093/nar/gkab271>.
- Venkatesham, M., Ayodhya, D., Madhusudhan, A., Babu, N. V. & Veerabhadram, G. 2014 A novel green one-step synthesis of silver nanoparticles using chitosan: catalytic activity and antimicrobial studies. *Applied Nanoscience* **4**, 113–119. <https://doi.org/10.1007/s13204-012-0180-y>.
- Waheed, S., Ahmad, A., Maqsood, S. K., Gul, S. & Jamil, T. 2014 Synthesis, characterization, permeation and antibacterial properties of cellulose acetate/polyethylene glycol membranes modified with chitosan. *Desalination* **351**, 59–69. <http://dx.doi.org/10.1016/j.desal.2014.07.019>.

- Wang, X., Lim, H. J. & Son, A. 2014 Characterization of denaturation and renaturation of DNA for DNA hybridization. *Environmental Health and Toxicity* **29**, 1–8. <https://doi.org/10.5620/eht.2014.29.e2014007>.
- Yanat, M. & Schroën, K. 2021 Preparation methods and applications of chitosan nanoparticles; with an outlook toward reinforcement of biodegradable packaging. *Reactive and Functional Polymers* **161**, 1–12. <https://doi.org/10.1016/j.reactfunctpolym.2021.104849>.

First received 20 November 2021; accepted in revised form 15 April 2022. Available online 23 April 2022